

Momentum-resolved spectral functions of SrVO₃ calculated by LDA+DMFT

I. A. Nekrasov,^{1,2} K. Held,³ G. Keller,² D. E. Kondakov,⁴ Th. Pruschke,⁵
M. Kollar,² O. K. Andersen,³ V. I. Anisimov,⁴ and D. Vollhardt²

¹*Institute for Electrophysics, Russian Academy of Sciences, Ekaterinburg, 620016, Russia*

²*Theoretical Physics III, Center for Electronic Correlations and Magnetism,
University of Augsburg, 86135 Augsburg, Germany*

³*Max-Planck Institute for Solid State Research,
Heisenbergstr. 1, 70569 Stuttgart, Germany*

⁴*Institute of Metal Physics, Russian Academy of Sciences, Ekaterinburg, 620219, Russia*

⁵*Institute for Theoretical Physics, University of Göttingen,
Tammannstr. 1, 37077 Göttingen, Germany*

Abstract

LDA+DMFT, the merger of density functional theory in the local density approximation and dynamical mean-field theory, has been mostly employed to calculate \mathbf{k} -integrated spectra accessible by photoemission spectroscopy. In this paper, we calculate \mathbf{k} -resolved spectral functions by LDA+DMFT. To this end, we employ the N th order muffin-tin (NMTO) downfolding to set up an effective low-energy Hamiltonian with three t_{2g} orbitals. This downfolded Hamiltonian is solved by DMFT yielding \mathbf{k} -dependent spectra. Our results show renormalized quasiparticle bands over a broad energy range from -0.7 eV to +0.9 eV with small “kinks”, discernible in the dispersion below the Fermi energy.

PACS numbers: 71.27.+a, 71.30.+h

I. INTRODUCTION

Transition metal oxides show a diversity of challenging physical phenomena, including superconductivity, metal-insulator transitions, and colossal magnetoresistance, and are therefore at the center of modern solid state research. Electrons in many of these materials are strongly correlated due to a large ratio of Coulomb interaction to bandwidth U/W , resulting in complicated many-electron physics which makes realistic calculations rather difficult. In particular, conventional bandstructure calculations, e.g., in the local density approximation (LDA)[1], fail because these effective one-particle approaches do not contain many-body physics like the formation of Hubbard bands, quasiparticle renormalization, and lifetime effects. In this respect LDA+DMFT, the recent merger [2–6] of LDA with the many-body dynamical mean-field theory (DMFT) [7–10], is a promising new approach which includes many-body aspects into realistic calculations. It has been successfully applied, in particular to calculate the total (\mathbf{k} -integrated) spectra of transition-metal oxides like LaTiO₃ [2, 11], V₂O₃ [12–14], Sr(Ca)VO₃ [14–20], LiV₂O₄ [21], Ca_{2-x}Sr_xRuO₄ [22, 23], CrO₂ [24], but also of Ni [25], Fe [25], and f -electron systems like Pu [26, 27] and Ce [28–33].

LDA+DMFT calculations for transition metal oxides have mostly been restricted to the d -bands around the Fermi energy, employing a simplified calculational scheme based on the LDA density of states (DOS) which holds for cubic systems [3]. Calculations with the full LDA Hamiltonian, including all $spdf$ valence orbitals in the DMFT have been performed for Pu [26, 27] and Ce [28–31]. Since the O_{2p}-Me_{3d} overlap is considerable for transition metal oxides, a full LDA Hamiltonian calculation should also take into account the rather large [34–36] oxygen-vanadium and oxygen-oxygen Coulomb interactions U_{pd} and U_p .

While a large number of interacting orbitals makes LDA+DMFT calculations with the full spd Hamiltonian difficult, they are feasible for the effective d -bands around the Fermi energy. To this end, a clear definition of the effective Hamiltonian for energies near the Fermi energy is mandatory. An accurate construction of this effective Hamiltonian is possible by the downfolding procedure for third generation muffin-tin orbitals (NMTOs) [37] and has recently been employed in the LDA+DMFT context by Pavarini *et al.* [17, 20]. Furthermore, Anisimov *et al.* [14] recently proposed a projection scheme of the Bloch functions onto a Wannier functions basis to obtain a few-orbital Hamiltonian. Such a downfolded or projected Hamiltonian is also required to calculate \mathbf{k} -resolved spectra.

Due to its simple crystal structure (cubic perovskite) and the $3d^1$ electronic configuration the transition metal oxide SrVO_3 is ideal for testing new theoretical methods for the realistic modeling of correlated materials. SrVO_3 is a strongly correlated metal with a pronounced lower Hubbard and quasiparticle peak in the photoemission spectra (PES) [38–40] as well as a pronounced quasiparticle and upper Hubbard band in the x-ray absorption spectrum [41]. After the substitution of Sr by Ca, PES [38] and Bremsstrahlung isochromat spectra (BIS) [42] originally suggested the onset of a Mott-Hubbard metal-insulator transition. By contrast, thermodynamic properties (Sommerfeld coefficient, resistivity, and paramagnetic susceptibility) [43] did not show significant effects upon Ca doping. An attempt to describe electronic properties of SrVO_3 by DMFT was made by Rozenberg *et al.* [44, 45] for the one-band Hubbard model using phenomenological parameters. Recently, the puzzling discrepancy between spectroscopic and thermal properties has been solved by new bulk-sensitive PES [39, 40, 46], showing similar spectra for CaVO_3 and SrVO_3 , in agreement with the thermodynamic results. This was confirmed theoretically by LDA+DMFT calculations [14, 16–20]. In this paper we present LDA+DMFT(QMC) calculations for SrVO_3 based on a NMTO downfolded effective Hamiltonian for three orbitals of t_{2g} symmetry crossing the Fermi energy. From this we calculate \mathbf{k} -resolved spectral functions and ARPES spectra. Recently angular-resolved photoemission spectroscopy (ARPES) on SrVO_3 was performed [47]; the data from Fujimori’s group [47] allow for the direct observation of the quasiparticle mass renormalization and band edge.

The paper is organized as follows. In Section II we briefly discuss the crystal structure and calculate the effective t_{2g} Hamiltonian for SrVO_3 by LDA/NMTO. In Section III, we discuss and compare two LDA+DMFT(QMC) calculations for SrVO_3 , based on this effective t_{2g} Hamiltonian and a simplified treatment using the DOS only. Finally, in Section IV the LDA+DMFT(QMC) calculated self-energy on the real axis $\Sigma(\omega)$ and \mathbf{k} -resolved spectral functions for SrVO_3 are presented. The paper is summarized in Section V.

II. CONSTRUCTION OF FEW-ORBITAL HAMILTONIANS

Starting point of a first principle calculation is usually the crystal structure. In our case, SrVO_3 is a perovskite with an ideal cubic $\text{Pm}\bar{3}\text{m}$ [48] symmetry, containing one V ion in the unit cell. This implies that the main structural element, the VO_6 octahedron, is not

distorted. The electronic configuration is $3d^1$, which follows from the formal oxidation V^{4+} . Due to the cubic symmetry, the d orbitals split into two sets: three t_{2g} and two e_g orbitals. In our case of an octahedral coordination with oxygen, the three-fold degenerated t_{2g} orbitals are lower in energy than the two-fold e_g orbitals. Since these t_{2g} and e_g bands do not overlap we will later restrict our calculation to an effective Hamiltonian with three t_{2g} orbitals filled with one electron per site.

For the LDA band structure calculations of $SrVO_3$ we first employed the LDA-LMTO(ASA) code version 47 which uses the basis of nonorthogonal linearized muffin-tin orbitals (LMTO; 2nd generation) in the atomic sphere approximation (ASA) [49]. Thereby, the partial waves were expanded to linear order in energy around the center of gravity of the filled part of the bands. The results are presented by thin solid lines in Fig. 1 and show $2p$ oxygen bands below -1.5 eV, three t_{2g} bands at the Fermi energy between -1.5 eV and 1.5 eV, and e_g bands between 1.5 eV and 6 eV. The other bands of our orbital basis set $[O(3s, 3d), V(4s, 4p), Sr(5s, 5p, 4d, 4f)]$ are empty and lie far above the Fermi level [50].

Secondly, with the same basis set we employed the third generation MTO, also known as N -th order muffin tin orbitals (NMTO) [37]. We expanded the MTO orbitals around the three points: -2.72 eV, 0.68 eV, and 6.8 eV. Here and in the following, all energies are measured relative to the Fermi energy at 0 eV. The NMTO results are shown as dashed lines in Fig. 1 and almost coincide with LMTOs in the region of interest, i.e., $O2p$ and $V3d$. The NMTO bands are found to be slightly lower in energy which is not surprising since 3rd generation MTOs have the proper energy dependence in the interstitial region and, moreover, more expansion points ($N + 1 = 4$) for the wave function than LMTOs where $N = 1$ (linear approach). For the high-lying empty bands, LMTO and NMTO bands are quite different; the NMTO bands are again lower in energy. As the third NMTO expansion point (6.8 eV) is in this region, we expect NMTOs to be more precise in this region than LMTOs, which are linearized at energies corresponding to the center of gravity of the *filled* parts of the bands. Hence, the LMTO expansion points are below the Fermi energy, far away from these high-lying empty bands. Moreover, the 2nd generation LMTOs have vanishing kinetic energy in the interstitial region.

A particular advantage of NMTOs is the possibility of calculating an effective (down-folded) Hamiltonian $\hat{H}^{\text{eff}}(\mathbf{k})$, confined to a reduced set of orbitals in a reduced window of energies. In the case of $SrVO_3$, the t_{2g} subset of the V $3d$ orbitals is of particular interest

as discussed above. Hence, we downfolded [37] to a 3×3 NMTO Hamiltonian $\hat{H}^{\text{eff}}(\mathbf{k})$ describing the three t_{2g} orbitals. For optimizing the energy window w.r.t. these orbitals, we chose two MTO expansion points, $\epsilon_0 = 0.41$ eV and $\epsilon_1 = 0.95$ eV, at the energy region of the t_{2g} bands. At these energies, the NMTOs span exactly the LDA eigenfunctions. Fig. 2 shows the eigenvalues of $\hat{H}^{\text{eff}}(\mathbf{k})$ along some high-symmetric directions in comparison with the NMTO results using the full orbital basis of Fig. 1. From the good agreement we conclude that $\hat{H}^{\text{eff}}(\mathbf{k})$ describes the three t_{2g} bands well. The slight discrepancy at the bottom of the band could have been avoided by choosing a smaller value of ϵ_0 . If we increase the number of these mesh points ϵ_i , the Hilbert space spanned by these NMTOs will converge to that spanned by the t_{2g} Wannier functions; the orthogonalization of these NMTOs will yield localized Wannier functions.

Fig. 3 compares the DOS of $\hat{H}^{\text{eff}}(\mathbf{k})$ obtained via tetrahedron integration [51] with the LMTO DOS. A minor difference to earlier calculations [16, 19] is that we used an orthogonal representation of the LMTO method in Refs. [16, 19], neglecting the so-called combined correction term. Because of this Refs. [16, 19] yield a slightly different t_{2g} bandshape with a discernibly reduction of the sharp peak at ≈ 1 eV. These differences are, however, small and unimportant for the final LDA+DMFT results. For the LMTO DOS of Fig. 3, we downfolded the band structure onto the t_{2g} states which, due to the oxygen $2p$ - t_{2g} hybridization, also have a contribution between -7 eV and -2 eV. Vice versa, downfolding to O- $2p$ states gives a contribution around the Fermi energy. To obtain the *effective* t_{2g} orbitals at the Fermi energy (which have primarily t_{2g} character with a small $2p$ admixture) we truncated the t_{2g} contribution in the oxygen region between -7 eV and -2 eV and renormalized the orbitals so that one has again one electron per site and orbital. Fig. 3 shows that the DOS calculated by this procedure resembles the downfolded NMTO DOS well. In particular, both DOSes have the same features and bandwidth. The agreement with the NMTO DOS of [17] is also very good.

III. LDA+DMFT CALCULATIONS USING DOWNFOLDING AND HILBERT TRANSFORM

In this Section, we will use two different methods to construct the non-interacting, i.e., kinetic energy part, of the three-band many-body problem: the NMTO downfolded t_{2g}

Hamiltonian $\hat{H}^{\text{eff}}(\mathbf{k})$ and the LMTO DOS of Fig. 3. This part of the Hamiltonian is then complemented by a local Coulomb interaction:

$$\begin{aligned} \hat{H} = \hat{H}_0^{\text{eff}} + U \sum_m \sum_i \hat{n}_{im\uparrow} \hat{n}_{im\downarrow} \\ + \sum_i \sum_{m \neq m'} \sum_{\sigma \sigma'} (U' - \delta_{\sigma \sigma'} J) \hat{n}_{im\sigma} \hat{n}_{im'\sigma'}. \end{aligned} \quad (1)$$

Here, the index i enumerates correlated lattice sites, m denotes orbitals, and σ the spin. \hat{H}_0^{eff} is a one-particle Hamiltonian generated from the LDA band structure where an averaged Coulomb interaction is subtracted to avoid double counting of the Coulomb interaction [2, 3]. The local intra-orbital Coulomb repulsion is denoted by U and the Hund's exchange coupling by J . Rotational invariance then fixes the local inter-orbital Coulomb repulsion $U' = U - 2J$, see, e.g., [52]. For three orbitals, U' equals the averaged Coulomb interaction \bar{U} [3, 11].

The Hamiltonian (1) is then solved by the recently developed LDA+DMFT approach [2] (for introductions see Refs. [3, 6], for reviews see Refs. [4, 5]). In this approach the solution of (1) is obtained by the dynamical mean-field theory (DMFT) [8–10], a non-perturbative many-body method based on the $d = \infty$ limit [7].

In this paper, \hat{H}_0^{eff} will be the NMTO downfolded (and symmetrically orthonormalized) Hamiltonian of Section II. The double counting correction is not relevant here since we consider only the three correlated t_{2g} orbitals [3, 11]. To calculate Coulomb interaction parameters appearing in (1) we previously [16, 19] employed the constrained LDA method [53], yielding an orbitally averaged Coulomb repulsion $\bar{U}=3.55$ eV and a Hund's exchange coupling $J=1.0$ eV.

In our LDA+DMFT calculations, we self-consistently solve the auxiliary DMFT impurity problem [8–10] by multi-band quantum Monte Carlo (QMC) simulations [54] together with the \mathbf{k} -integrated Dyson equation:

$$\mathbf{G}(\omega) = \int_{\text{BZ}} d\mathbf{k} [\omega + \mu - \Sigma(\omega) - \mathbf{h}_0^{\text{eff}}(\mathbf{k})]^{-1}. \quad (2)$$

Here, $\mathbf{G}(\omega)$, $\Sigma(\omega)$, and $\mathbf{h}_0^{\text{eff}}(\mathbf{k})$ are 3×3 matrices in orbital space, denoting the Green function, self-energy, and the downfolded NMTO Hamiltonian \hat{H}_0^{eff} in reciprocal space, respectively; μ is the chemical potential. Since QMC is formulated on the imaginary axis, we employed Eq. (2) for Matsubara frequencies and analytically continued $G(\omega)$ to real frequencies by means of the maximum entropy method [55].

In our previous calculations [16, 19], we used a simplified scheme based on the LDA DOS only. Within a cubic symmetry, the local DMFT self-energy becomes diagonal and even orbital-independent: $\Sigma_{mm'\sigma\bar{\sigma}}(\omega) = \delta_{mm'}\delta_{\sigma\bar{\sigma}}\Sigma(\omega)$. Then, the Green functions $G(\omega)$ of the lattice problem can be expressed via the Hilbert transform of the LDA DOS $N^0(\epsilon)$:

$$G(\omega) = \int d\epsilon \frac{N^0(\epsilon)}{\omega + \mu - \epsilon - \Sigma(\omega) + i\eta}, \quad (3)$$

instead of Eq. (2).

In Fig. 4, we present a comparison between one-particle LDA+DMFT(QMC) spectra for SrVO₃ obtained by using Eq. (3) with the Vanadium t_{2g} LDA DOS (thin solid line in Fig. 3; calculated as described in Section II) and Eq. (2) with $\mathbf{h}_0^{\text{eff}}(\mathbf{k})$. Both methods give the same results, as is to be expected for a cubic system. One can see the generic “three-peak” spectrum of a strongly correlated metal: the quasiparticle peak slightly above the Fermi energy, and lower and upper Hubbard bands to the left and right. The results presented here agree well with those reported in Refs. [14, 16–20]. The LDA+DMFT calculations of Ref. [15], with a focus on bulk surface differences, used a somewhat lower Coulomb interaction $\bar{U} = U - 2J = 2.6, 2.9$ eV.

IV. CALCULATION OF \mathbf{k} -RESOLVED SPECTRA

The purpose of this paper is to calculate the \mathbf{k} -resolved spectral function $A(\mathbf{k}, \omega)$ for SrVO₃ within the LDA+DMFT(QMC) scheme. Here,

$$A(\mathbf{k}, \omega) = -\frac{1}{\pi} \text{ImTr} \mathbf{G}(\mathbf{k}, \omega) \quad (4)$$

is determined by the diagonal elements of the Green function matrix in orbital space

$$\mathbf{G}(\mathbf{k}, \omega) = [\omega - \Sigma(\omega) - \mathbf{h}_0^{\text{eff}}(\mathbf{k})]^{-1}. \quad (5)$$

From this definition one can see that the two necessary ingredients to calculate $A(\mathbf{k}, \omega)$ are (i) the Hamiltonian matrix $\mathbf{h}_0^{\text{eff}}(\mathbf{k})$, and (ii) the self-energy matrix $\Sigma(\omega)$ at real frequencies. Similar schemes were recently used by Liebsch and Lichtenstein to compute quasiparticle properties of Sr₂RuO₄ [22] and by Biermann *et al.* to describe the presence of a lower Hubbard band in γ -Mn [56]. Angle-resolved photoemission spectra of the 2D Hubbard model were also investigated by Maier *et al.* [57] in the framework of the dynamical cluster

approximation (DCA) [58] and by Sadovskii *et al.* [59] within the so-called DMFT+ $\Sigma_{\mathbf{k}}$ approach. Within DMFT the self-energy on the real axis was also calculated in [14, 60].

In our case of cubic symmetry, $\Sigma(\omega)$ is the same for all t_{2g} orbitals. Eqs. (2)-(5) are formulated in terms of a self-energy $\Sigma(\omega)$ for *real* frequencies ω . Since LDA+DMFT(QMC) determines the self-energy $\Sigma(i\omega_n)$ for Matsubara frequencies $i\omega_n$, the calculation of $\Sigma(\omega)$ requires a separate calculation. To this end we first employ the maximum entropy method [55] to obtain the \mathbf{k} -integrated, spectral function $A(\omega) = -\frac{1}{\pi}\text{Im}G(\omega)$ with $G(\omega) \equiv (\mathbf{G}(\omega))_{mm}$, shown in Fig. 4. The Kramers-Kronig relation

$$\text{Re}G(\omega) = -\frac{1}{\pi} \int_{-\infty}^{\infty} d\omega' \frac{\text{Im}G(\omega')}{\omega - \omega' + i\eta} \quad (6)$$

then determines the real part of the Green function. The complex Green function and the complex self-energy are related by the \mathbf{k} -integrated Dyson Eq. (2). We obtain the self-energy as the numerical solution of Eq. (2).

Fig. 5 presents the resulting real and imaginary parts of the self-energy $\Sigma(\omega)$ as a function of real frequencies ω . The calculated self-energy satisfies the Kramers-Kronig relation

$$\text{Re}\Sigma(\omega) = -\frac{1}{\pi} \int_{-\infty}^{\infty} d\omega' \frac{\text{Im}\Sigma(\omega')}{\omega - \omega'} + \text{constant}. \quad (7)$$

The self-energy is highly asymmetric with respect to the Fermi level, as expected for the present case of an asymmetric LDA DOS and 1/6 band filling. At the energies $\omega \sim \pm 1.5$ eV the real part of the self-energy, $\text{Re}\Sigma$, has extrema, originating from the crossover from the central quasiparticle peak to the lower and upper Hubbard bands. The two extrema of $\text{Im}\Sigma$, which coincide with zeros of $\text{Re}\Sigma$, are responsible for the strong incoherence of the lower and upper Hubbard bands (see Fig. 4).

Let us now turn from the Hubbard bands to the energy regime of the central (quasiparticle) peak, ranging from about -0.8 eV to 1.4 eV in Fig. 4. From a coarse grained perspective, the imaginary part of the self-energy $\text{Im}\Sigma(\omega)$ is still (relatively) small in this regime and the real part of the self-energy can very roughly be described by a straight line (dashed line in Fig. 5, main panel). This line corresponds to a quasiparticle weight $Z = m^*/m = 1 - \frac{\partial \text{Re}\Sigma(\omega)}{\partial \omega}|_{\omega=0} = 1.9$, a value which is in accord with the one determined from the lowest Matsubara frequency ω_0 , i.e., $m^*/m = 1 - \frac{\text{Im}\Sigma(\omega_0)}{\omega_0} \approx 2$, and the estimate from the overall weight of the central (quasiparticle) peak (from -0.8 eV to 1.4 eV:

$1/Z = m^*/m \approx 2.2$). It is also very close to the value $m^*/m = 2.2$ obtained in Ref. [17, 20] and the value $m^*/m = 1.8 \pm 0.2$ from more recent ARPES experiments [47].

But the inset of Fig. 5 reveals that, strictly speaking, the Fermi liquid regime with $\text{Im}\Sigma(\omega) \sim -\omega^2$ and $\text{Re}\Sigma(\omega) \sim -\omega$ only extends from -0.2 up to 0.15 eV. The slope of $\text{Re}\Sigma(\omega)$ is steeper here than the slope of the coarse grained line of the main panel of Fig. 5. Hence, the strict (low-energy) Fermi-liquid mass enhancement is somewhat larger than $m^*/m = 1.9$: The effective mass in this low energy (low E) regime is obtained as $m_{\text{low}E}^*/m = 3$ from the dashed line of the inset.

Next to this Fermi liquid regime, there are pronounced shoulders in $\text{Re}\Sigma(\omega)$ at $\omega = -0.25$ eV and $+0.25$ eV, with corresponding structures in $\text{Im}\Sigma(\omega)$, according to the Kramers-Kronig relation (7). These shoulders of $\text{Re}\Sigma(\omega)$ will become important in the context of the quasiparticle dispersion in Fig. 8. For $\text{Im}\Sigma(\omega)$, similar structures were reported in [60], based on LDA+DMFT(QMC) calculations for LaTiO_3 [11]. Because of the above-mentioned shoulders in $\text{Re}\Sigma(\omega)$, $\text{Re}\Sigma(\omega)$ can be roughly approximated by a straight line (dashed line of the main panel Fig. 5) in the overall energy regime of the central quasiparticle peak.

With the knowledge of the self-energy on the real axis, we are now in the position to calculate the \mathbf{k} -resolved spectral functions Eqs. (4)-(5) and the quasiparticle dispersion. In Fig. 6, the LDA+DMFT(QMC) spectral functions $A(\mathbf{k}, \omega)$ for SrVO_3 are presented. In the energy regions [-3 eV, -1 eV] and [1.5 eV, 5 eV] there is some broad, non-dispersive spectral weight corresponding to the incoherent lower and upper Hubbard bands. Around the Fermi energy, $A(\mathbf{k}, \omega)$ shows a dispersive peak which is somewhat smeared out away from the Fermi energy because of lifetime effects, $\tau^{-1} \sim \omega^2$; the inset of Fig. 7 shows a magnification in the vicinity of the Fermi energy.

The \mathbf{k} -resolved spectral functions in turn allow us to determine the LDA+DMFT(QMC) quasiparticle bands, which are shown as dots in Fig. 8 and compared to the bare LDA bands (solid lines). These dots are the maxima of the spectral function from Figs. 6 and 7 around the Fermi level where the quasiparticles are well defined. They resemble the LDA dispersion, albeit renormalized. This is to be expected for a Fermi liquid, where

$$\mathbf{G}(\omega) = Z \int_{\text{BZ}} d\mathbf{k} [\omega + Z\mu - Z\mathbf{h}_0^{\text{eff}}(\mathbf{k})]^{-1} \quad (8)$$

in the quasiparticle region. Employing this Fermi liquid behavior, and using $1/Z = 1.9$, we can reconstruct the band-structure directly from the LDA spectrum. As seen from Fig. 8, the

result (dashed curves) agrees well with the quasiparticle bands (dots). However it should be noted that changes in slope of the LDA+DMFT(QMC) dispersion occur at $\omega = -0.25$ eV and (hardly discernible) $\omega = +0.25$ eV (see Fig. 8). These “kinks” [61, 62] stem from the shoulders in the real part of the self-energy (Fig. 5) and will be discussed in detail elsewhere [63]. Strong interest in kinks of the dispersion has followed their observation in various high- T_c superconductors [64], where they have been attributed mainly to phonons. In electronic systems kinks in the dispersion have also been found in theoretical studies of the 2D Hubbard model within the fluctuation exchange approximation [65] and most recently within the self-consistent projection operator method [66].

When comparing with experiments, we note that for *\mathbf{k} -resolved* spectra the influence of PES matrix elements may be stronger than for the *\mathbf{k} -integrated* spectra. Nevertheless, their inclusion affects the relative intensities but not their position. We find qualitative agreement with recent ARPES dispersions [47], where the renormalized band structure was observed directly. In particular, we see from Fig. 8 that the bottom of the quasiparticle band is located at approximately $\omega = -0.7$ eV, in contrast to the LDA value of $\omega = -1.2$ eV.

V. CONCLUSION

In this paper, we presented LDA+DMFT(QMC) computations of *\mathbf{k} -resolved* spectral functions of SrVO₃. The necessary input is an LDA-calculated Hamiltonian \hat{H}_0^{eff} and the LDA+DMFT self-energy at real frequencies $\Sigma(\omega)$. We used the NMTO downfolding to calculate \hat{H}_0^{eff} for the strongly correlated V-3d(t_{2g}) orbitals of SrVO₃ crossing the Fermi energy. This calculation gives essentially the same *\mathbf{k} -integrated* spectrum as our previous calculations [16, 19] based on the t_{2g} projected DOS.

The LDA+DMFT *\mathbf{k} -resolved* spectral function shows two incoherent Hubbard bands and dispersive quasiparticle bands. The latter resembles the LDA dispersion which from a coarse grained perspective is just normalized by $m^*/m=1.9$ all the way from the lower band edge to the Fermi energy to the upper band edge of the central (quasiparticle) peak. This m^*/m agrees with ARPES experiments [47]. On a finer scale we note however deviations: First, the Fermi liquid regime only extends from -0.2 eV to 0.15 eV, strictly speaking. In this low energy regime, the effective mass is somewhat higher ($m_{\text{low}E}^*/m \approx 3$). Second, following this strict Fermi liquid regime the imaginary part of the self-energy stays (relatively) small, while

the real part develops a shoulder. This shoulder translates into a “kink” in the dispersion.

VI. ACKNOWLEDGMENTS

We thank J. W. Allen, J. Fink, P. Fulde, D. Manske, K. Matho, and Y.-f. Yang for helpful discussions. This work was supported by Russian Basic Research Foundation grant RFFI-GFEN-03-02-39024_a (VA,IN,DK), RFFI-04-02-16096 (VA,IN,DK), RFFI-05-02-17244 (IN), RFFI-05-02-16301 (IN) and the Deutsche Forschungsgemeinschaft through Sonderforschungsbereich 484 (DV,GK,MK,IN) and in part by the joint UrO-SO project N22 (VA,IN), the Emmy-Noether program (KH), and programs of the Presidium of the Russian Academy of Sciences (RAS) “Quantum macrophysics” and of the Division of Physical Sciences of the RAS “Strongly correlated electrons in semiconductors, metals, superconductors and magnetic materials”. One of us (IN) acknowledges Dynasty Foundation and International Center for Fundamental Physics in Moscow program for young scientists 2005, Russian Science Support Foundation program for young PhD of Russian Academy of Science 2005.

-
- [1] R. O. Jones and O. Gunnarsson, *Rev. Mod. Phys.* **61**, 689 (1989).
 - [2] V. I. Anisimov, A. I. Poteryaev, M. A. Korotin, A. O. Anokhin, and G. Kotliar, *J. Phys. Cond. Matter* **9**, 7359 (1997); A. I. Lichtenstein, and M. I. Katsnelson, *Phys. Rev. B* **57**, 6884 (1998).
 - [3] K. Held, I. A. Nekrasov, N. Blümer, V. I. Anisimov, and D. Vollhardt, *Int. J. Mod. Phys. B* **15**, 2611 (2001).
 - [4] K. Held, I. A. Nekrasov, G. Keller, V. Eyert, N. Blümer, A. K. McMahan, R. T. Scalettar, Th. Pruschke, V. I. Anisimov, and D. Vollhardt, *Psi-k Newsletter* **56**, 65 (2003), http://psi-k.dl.ac.uk/newsletters/News_56/Highlight_56.pdf.
 - [5] A. I. Lichtenstein, M. I. Katsnelson, G. Kotliar, in *Electron Correlations and Materials Properties 2nd ed.*, edited by A. Gonis, Nicholis Kioussis, and Mikael Ciftan, Kluwer Academic/Plenum, p. 428, New York (2002), available as cond-mat/0112079.
 - [6] G. Kotliar and D. Vollhardt, *Physics Today* **57**, No. 3 (March), 53 (2004).
 - [7] W. Metzner and D. Vollhardt, *Phys. Rev. Lett.* **62**, 324 (1989).

- [8] D. Vollhardt, in *Correlated Electron Systems*, edited by V. J. Emery, World Scientific, Singapore, 1993, p. 57.
- [9] Th. Pruschke, M. Jarrell, and J. K. Freericks, *Adv. in Phys.* **44**, 187 (1995).
- [10] A. Georges, G. Kotliar, W. Krauth, and M. J. Rozenberg, *Rev. Mod. Phys.* **68**, 13 (1996).
- [11] I. A. Nekrasov, K. Held, N. Blümer, A. I. Poteryaev, V. I. Anisimov, and D. Vollhardt, *Eur. Phys. J. B* **18**, 55 (2000).
- [12] K. Held, G. Keller, V. Eyert, D. Vollhardt, and V. I. Anisimov, *Phys. Rev. Lett.* **86**, 5345 (2001); S. -K. Mo, H.-D. Kim, J. W. Allen, G.-H. Gweon, J. D. Denlinger, J.-H. Park, A. Sekiyama, A. Yamasaki, S. Suga, P. Metcalf, and K. Held, *Phys. Rev. Lett.*, **93**, 076404 (2004); G. Keller, K. Held, V. Eyert, D. Vollhardt, and V. I. Anisimov, *Phys. Rev. B* **70**, 205116 (2004).
- [13] M. S. Laad, L. Craco, and E. Müller-Hartmann, *Phys. Rev. Lett.* **91**, 156402 (2003).
- [14] V. I. Anisimov, D. E. Kondakov, A. V. Kozhevnikov, I. A. Nekrasov, Z. V. Pchelkina, J. W. Allen, S.-K. Mo, H.-D. Kim, P. Metcalf, S. Suga, and A. Sekiyama, G. Keller, I. Leonov, X. Ren, D. Vollhardt, *Phys. Rev. B* **71**, 125119 (2005).
- [15] A. Liebsch, *Phys. Rev. Lett.* **90**, 096401 (2003).
- [16] I. A. Nekrasov, G. Keller, D. E. Kondakov, A. V. Kozhevnikov, Th. Pruschke, K. Held, D. Vollhardt, and V. I. Anisimov, cond-mat/0211508, superceded by [18].
- [17] E. Pavarini, S. Biermann, A. Poteryaev, A. I. Lichtenstein, A. Georges, O. K. Andersen, *Phys. Rev. Lett.* **92**, 176403 (2004).
- [18] A. Sekiyama, H. Fujiwara, S. Imada, S. Suga, H. Eisaki, S. I. Uchida, K. Takegahara, H. Harima, Y. Saitoh, I. A. Nekrasov, G. Keller, D. E. Kondakov, A. V. Kozhevnikov, Th. Pruschke, K. Held, D. Vollhardt, and V. I. Anisimov, *Phys. Rev. Lett.* **93**, 156402 (2004).
- [19] I. A. Nekrasov, G. Keller, D. E. Kondakov, A. V. Kozhevnikov, Th. Pruschke, K. Held, D. Vollhardt, and V. I. Anisimov, cond-mat/0501240, *Phys. Rev. B*, in print.
- [20] E. Pavarini, A. Yamasaki, J. Nuss, and O. K. Andersen, cond-mat/0504034.
- [21] I. A. Nekrasov, Z. V. Pchelkina, G. Keller, Th. Pruschke, K. Held, A. Krimmel, D. Vollhardt, and V. I. Anisimov, *Phys. Rev. B* **67**, 085111 (2003).
- [22] A. Liebsch and A. Lichtenstein, *Phys. Rev. Lett.* **84**, 1591 (2000).
- [23] V. I. Anisimov, I. A. Nekrasov, D. E. Kondakov, T. M. Rice, and M. Sigrist, *Eur. Phys. J. B* **25**, 191 (2002).

- [24] L. Craco, M. S. Laad, and E. Müller-Hartmann, Phys. Rev. Lett. **90**, 237203 (2003).
- [25] A. I. Lichtenstein, M. I. Katsnelson, and G. Kotliar, Phys. Rev. Lett. **87**, 67205 (2001).
- [26] S. Y. Savrasov, G. Kotliar, and E. Abrahams, Nature **410**, 793 (2001).
- [27] S. Y. Savrasov and G. Kotliar, Phys. Rev. B **69**, 245101 (2004).
- [28] M. B. Zöfl, I. A. Nekrasov, Th. Pruschke, V. I. Anisimov, and J. Keller, Phys. Rev. Lett. **87**, 276403 (2001).
- [29] K. Held, A. K. McMahan, and R. T. Scalettar, Phys. Rev. Lett. **87**, 276404 (2001).
- [30] A. K. McMahan, K. Held, and R. T. Scalettar, Phys. Rev. B **67**, 75108 (2003).
- [31] K. Haule, V. Oudovenko, S. Y. Savrasov, and G. Kotliar Phys. Rev. Lett. **94**, 036401 (2005),
- [32] A. K. McMahan, cond-mat/0504380.
- [33] B. Amadon, S. Biermann, A. Georges, and F. Aryasetiawan, cond-mat/0504732.
- [34] A. K. McMahan, R. M. Martin, and S. Satpathy, Phys. Rev. B **38**, 6650 (1988).
- [35] M. S. Hybertsen, M. Schlüter, and N. E. Christensen, Phys. Rev. B **39**, 9028 (1989).
- [36] M. L. Knotek and P. J. Feibelman, Phys. Rev. Lett. **40**, 964 (1978).
- [37] O. K. Andersen and T. Saha-Dasgupta, Phys. Rev. B **62**, R16219 (2000); O. K. Andersen, T. Saha-Dasgupta, S. Ezhov, L. Tsetseris, O. Jepsen, R. W. Tank, C. Arcangeli, and G. Krier, Psi-k Newsletter **45**, 86 (2001); O. K. Andersen, T. Saha-Dasgupta, and S. Ezhov, Bull. Mater. Sci. **26**, 19 (2003).
- [38] A. Fujimori, I. Hase, H. Namatame, Y. Fujishima, Y. Tokura, H. Eisaki, S. Uchida, K. Takegahara, and F. M. F. de Groot, Phys. Rev. Lett. **69**, 1796 (1992).
- [39] K. Maiti, D. D. Sarma, M. J. Rozenberg, I. H. Inoue, H. Makino, O. Goto, M. Pedio, and R. Cimino, Europhys. Lett. **55**, 246 (2001).
- [40] A. Sekiyama, H. Fujiwara, S. Imada, S. Suga, H. Eisaki, S. I. Uchida, K. Takegahara, H. Harima, and Y. Saitoh, cond-mat/0206471, superceded by [18].
- [41] I. H. Inoue, I. Hase, Y. Aiura, A. Fujimori, K. Morikawa, T. Mizokawa, Y. Haruyama, T. Maruyama, and Y. Nishihara, Physica C **235-240**, 1007 (1994).
- [42] K. Morikawa, T. Mizokawa, K. Kobayashi, A. Fujimori, H. Eisaki, S. Uchida, F. Iga, and Y. Nishihara, Phys. Rev. B **52**, 13711 (1995).
- [43] Y. Aiura, F. Iga, Y. Nishihara, H. Ohnuki, H. Kato, Phys. Rev. B **47**, 6732 (1993); I. H. Inoue, I. Hase, Y. Aiura, A. Fujimori, Y. Haruyama, T. Maruyama, and Y. Nishihara, Phys. Rev. Lett. **74**, 2539 (1995); I. H. Inoue, O. Goto, H. Makino, N. E. Hussey, and M. Ishikawa,

- Phys. Rev. B **58**, 4372 (1998).
- [44] M. J. Rozenberg, I. H. Inoue, H. Makino, F. Iga, and Y. Nishihara, Phys. Rev. Lett. **76**, 4781 (1996).
- [45] H. Makino, I. H. Inoue, M. J. Rozenberg, I. Hase, Y. Aiura, and S. Onari, Phys. Rev. B **58**, 4384 (1998).
- [46] R. Eguchi, T. Kiss, S. Tsuda, T. Shimojima, T. Yokoya, A. Chainani, S. Shin, I. H. Inoue, T. Togashi, S. Watanabe, C. Q. Zhang, C. T. Chen, M. Arita, K. Shimada, H. Namatame, and M. Taniguchi, cond-mat/0504576.
- [47] T. Yoshida, K. Tanaka, H. Yagi, A. Ino, H. Eisaki, A. Fujimori, and Z.-X. Shen, cond-mat/0504075.
- [48] M. J. Rey, P. H. Dehaudt, J. C. Joubert, B. Lambert-Andron, M. Cyrot, and F. Cyrot-Lackmann, J. Solid State Chem. **86**, 101 (1990).
- [49] O. K. Andersen and O. Jepsen, Phys. Rev. Lett. **53**, 2571 (1984); The Stuttgart TB-LMTO-ASA Program, <http://www.fkf.mpg.de/andersen/LMTODOC/LMTODOC.html>.
- [50] Our results are in agreement with LDA calculations within the LMTO-ASA method by S. Itoh, Solid State Communications, **88**, 525 (1993), and those by J. Takegahara, Electron Spectrosc. Relat. Phenom. **66**, 303 (1995) in the basis of augmented plane waves (APW). For our purposes, i.e., for the combination of the LDA band structure with DMFT [2], the atomic-like wave functions basis set of the MTO method is however more appropriate.
- [51] Ph. Lambin and J. P. Vigneron, Phys. Rev. B **29**, 3430 (1984); O. Jepsen and O. K. Andersen, Solid State Commun. **9**, 1763 (1971); P. E. Blöchl, O. Jepsen, and O. K. Andersen, Phys. Rev. B **49**, 16223 (1994).
- [52] M. B. Zöfl, Th. Pruschke, J. Keller, A. I. Poteryaev, I. A. Nekrasov, and V. I. Anisimov, Phys. Rev. B **61**, 12810 (2000).
- [53] O. Gunnarsson, O. K. Andersen, O. Jepsen, and J. Zaanen, Phys. Rev. B **39**, 1708 (1989).
- [54] J. E. Hirsch and R. M. Fye, Phys. Rev. Lett. **56**, 2521 (1986). For multi-band QMC within DMFT see [3].
- [55] For a review of the maximum entropy method see M. Jarrell and J. E. Gubernatis, Physics Reports **269**, 133 (1996).
- [56] S. Biermann, A. Dallmeyer, C. Carbone, W. Eberhardt, C. Pampuch, O. Rader, M. I. Katsnelson, and A. I. Lichtenstein, JETP Letters **80**, 612 (2005).

- [57] Th. A. Maier, Th. Pruschke, and M. Jarrell, Phys. Rev. B **66**, 075102 (2002).
- [58] For a review of DCA see Th. Maier, M. Jarrell, Th. Pruschke, M. H. Hettler, “Quantum Cluster Theories”, cond-mat/0404055, (submitted to Rev. Mod. Phys.).
- [59] M. V. Sadovskii, I. A. Nekrasov, E. Z. Kuchinskii, Th. Pruschke, V. I. Anisimov, cond-mat/0502612; E. Z. Kuchinskii, I. A. Nekrasov, and M. V. Sadovskii, cond-mat/0506215, JETP Letters, in print.
- [60] N. Blümer, Ph. D. thesis, Universität Augsburg, 2002.
- [61] We thank J. Fink for useful discussions regarding these kinks during the 8th Japanese-German Symposium on *Competing Phases in Novel Condensed Matter Systems*, Lauterbad, August 2004, where our results were first presented. We also thank him and P. Fulde for useful discussions at the International Workshop on *Strong Correlations and ARPES: Recent Progress in Theory and Experiment*, Max-Planck Institute for Physics of Complex Systems, Dresden, April 2005.
- [62] G. Keller, D. E. Kondakov, I. Nekrasov, K. Held, T. Pruschke, V. I. Anisimov, and D. Vollhardt, International Conference on Strongly Correlated Electron Systems SCES '04, Abstract Booklet WE-TMO3-55, p.131; G. Keller, V. I. Anisimov, D. E. Kondakov, A. V. Kozhevnikov, I. A. Nekrasov, Z. V. Pchelkina, I. Leonov, X. Ren, and D. Vollhardt, Verhandl. DPG (VI) 40, 2/2005, TT 16.87, p. 580.
- [63] I. Nekrasov *et al.*, to be published.
- [64] A. Lanzara *et al.*, Nature **412**, 510 (2001). For reviews see T. Cuk, D. H. Lu, X. J. Zhou, Z.-X. Shen, T. P. Deveraux, and N. Nagaosa, phys. stat. sol. (b) **242**, 11 (2005); A. Damascelli, Z. Hussain, and Z.-X. Shen, Rev. Mod. Phys. **75**, 473 (2003).
- [65] D. Manske, I. Eremin, and K. H. Bennemann, Phys. Rev. Lett. **87**, 177005 (2001); Phys. Rev. B **67**, 134520 (2003).
- [66] Y. Kakehashi and P. Fulde, cond-mat/0507564.

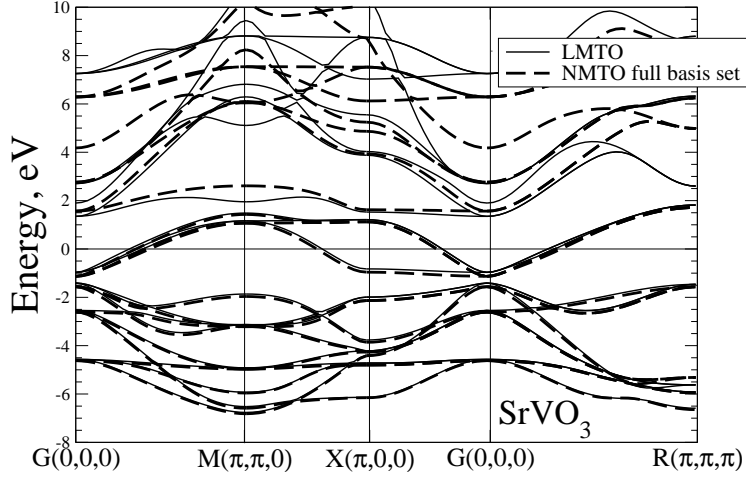


FIG. 1: Comparison of the LDA band structure of SrVO_3 calculated by LMTO (thin solid line) and NMTO (dashed line) for the full orbital basis set. Here, and in the following figures, the Fermi energy corresponds to zero energy.

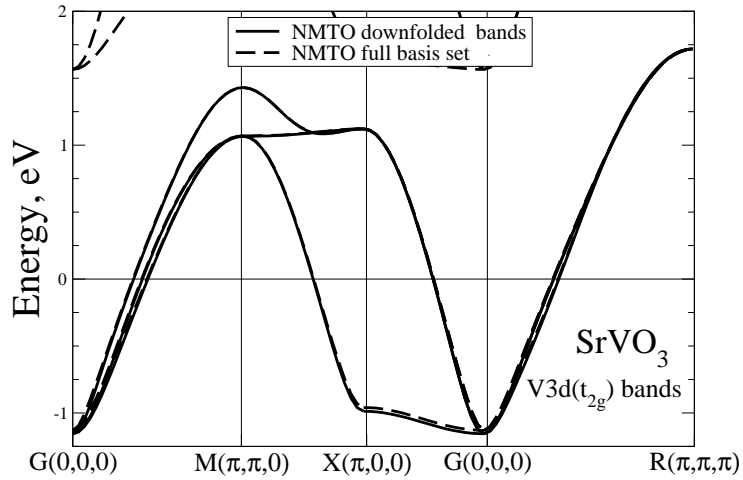


FIG. 2: Comparison of the NMTO downfolded t_{2g} bands (full line) with NMTO for the full orbital basis set (dashed line).

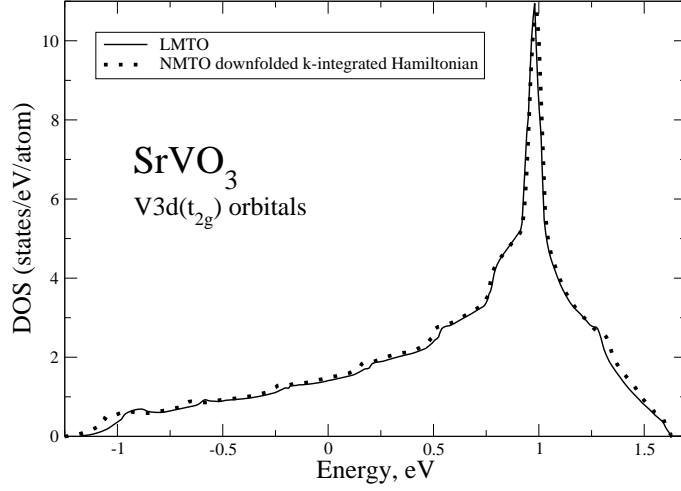


FIG. 3: Comparison of the t_{2g} DOS calculated (i) by LMTO as explained in the text (thin solid line) and (ii) by integrating the down-folded NMTO Hamiltonian over the Brillouin zone (dotted line).

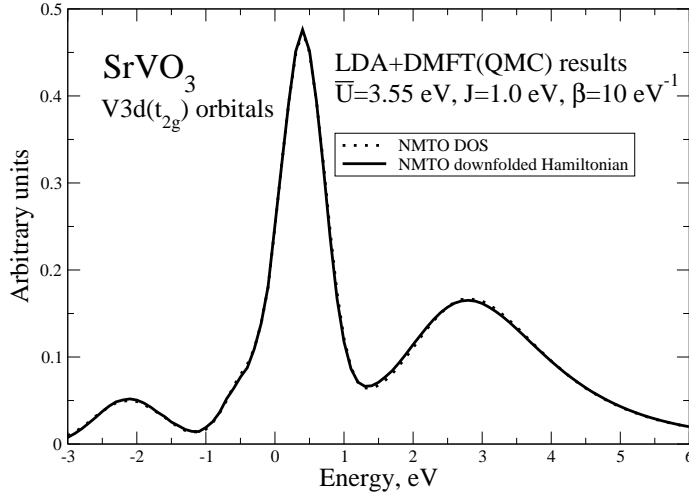


FIG. 4: Comparison of the LDA+DMFT(QMC) \mathbf{k} -integrated SrVO_3 spectrum of the three t_{2g} bands crossing the Fermi energy obtained by NMTO (dotted line) and by the NMTO downfolded t_{2g} Hamiltonian (full line), respectively. The local Coulomb interaction was calculated by constrained LDA as $\bar{U}=3.55$ eV and $J=1.0$ eV; the temperature is 0.1 eV.

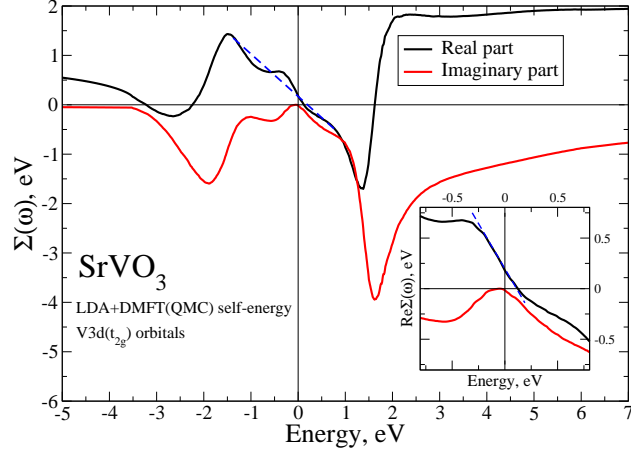


FIG. 5: Real (black line) and imaginary (gray line) parts of the LDA+DMFT(QMC) self-energy $\Sigma(\omega)$ for the vanadium t_{2g} orbitals of SrVO_3 (see text). The inset shows the magnification of $\text{Re}\Sigma(\omega)$ and $\text{Im}\Sigma(\omega)$ near the Fermi level. The dashed lines indicate a coarse grained linearization for the whole range of the central peak (-0.8 to 1.4 eV; main figure) and for the strict quasiparticle regime from -0.2 eV to $+0.15$ eV (inset).

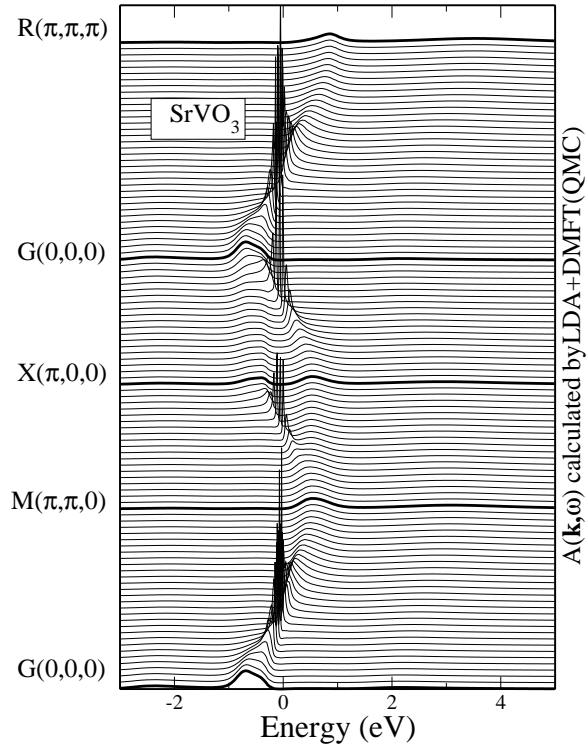


FIG. 6: Spectral function $A(\mathbf{k}, \omega)$ for the three V-3d(t_{2g}) bands of SrVO₃ as calculated by LDA+DMFT(QMC).

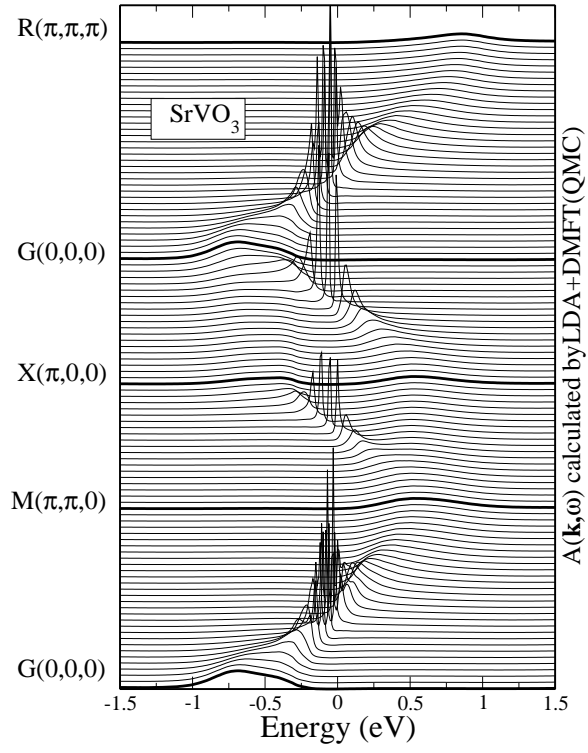


FIG. 7: Magnification of Fig. 6 around the Fermi energy (0 eV).

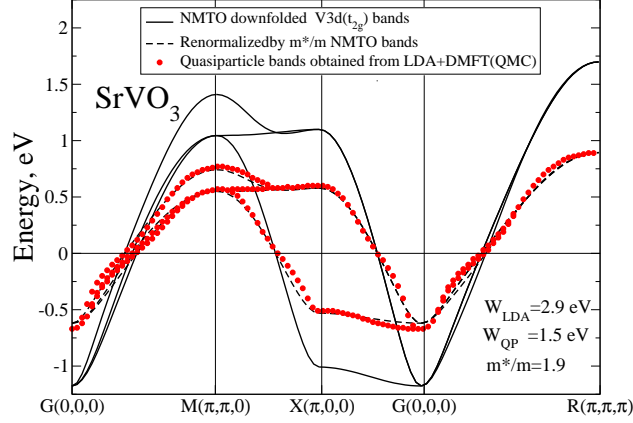


FIG. 8: LDA+DMFT(QMC) dispersion for SrVO₃ (dots) compared with LMTO (full line) and quasiparticle renormalization of the LMTO dispersion by $Z = 1/1.9$ (dashed line). The ratio of bandwidths yields $1/Z = m^*/m = 1.9$. The dashed line represents a simple quasiparticle renormalization of the NMTO bands by $1/Z = 1.9$. At $\omega = -0.25 \text{ eV}$, we see a “kink” in the LDA+DMFT(QMC) dispersion (dots), clearly discernible as a deviation from the simple renormalized LDA bands (dashed line).